OXFORD

Briefings in Bioinformatics, 2025, **26(1)**, bbaf059

https://doi.org/10.1093/bib/bbaf059

Case Study

Longitudinal urine metabolic profiling and gestational age prediction in human pregnancy

Xiaotao Shen [1,2,3,‡], Songjie Chen [1,4,‡], Liang Liang [1,5,‡], Monika Avina [1], Hanyah Zackriah [6], Laura Jelliffe-Pawlowski [7,8], Larry Rand [8,*], Michael P. Snyder [1,*]

[1]Genetics Department, Stanford University School of Medicine, 300 Pasteur Drive, Stanford, California 94305, USA
[2]Lee Kong Chian School of Medicine, Nanyang Technological University, 59 Nanyang Drive, Singapore 636921, Singapore
[3]School of Chemistry, Chemical Engineering and Biotechnology, Nanyang Technological University, 62 Nanyang Drive, Singapore 637459, Singapore
[4]Merck & Co., Inc., 213 East Grand Avenue, South San Francisco, CA 94080, USA
[5]Department of Obstetrics and Gynecology and Biochemistry, Medical College of Wisconsin, 8701 Watertown Plank Road, Wauwatosa, Wisconsin 53226, USA
[6]Department of Molecular and Cell Biology, University of California, Berkeley, 142 Weill Hall, Berkeley, CA 94720-3200, USA
[7]Rory Meyers College of Nursing, New York University, 433 First Avenue, New York, NY 10010, USA
[8]School of Medicine, University of California, San Francisco, 513 Parnassus Avenue, San Francisco, CA 94143, USA

*Corresponding authors. Larry Rand, University of California San Francisco. E-mail: larry.rand@ucsf.edu; Michael P. Snyder, Stanford University School of Medicine, Genetics. E-mail: mpsnyder@stanford.edu

‡Xiaotao Shen, Songjie Chen, and Liang Liang contributed equally.

Abstract

Pregnancy is a vital period affecting both maternal and fetal health, with impacts on maternal metabolism, fetal growth, and long-term development. While the maternal metabolome undergoes significant changes during pregnancy, longitudinal shifts in maternal urine have been largely unexplored. In this study, we applied liquid chromatography–mass spectrometry-based untargeted metabolomics to analyze 346 maternal urine samples collected throughout pregnancy from 36 women with diverse backgrounds and clinical profiles. Key metabolite changes included glucocorticoids, lipids, and amino acid derivatives, indicating systematic pathway alterations. We also developed a machine learning model to accurately predict gestational age using urine metabolites, offering a non-invasive pregnancy dating method. Additionally, we demonstrated the ability of the urine metabolome to predict time-to-delivery, providing a complementary tool for prenatal care and delivery planning. This study highlights the clinical potential of urine untargeted metabolomics in obstetric care.

Keywords: pregnancy; urine metabolomics; gestational age prediction

Introduction

Accurate gestational age (GA) dating is essential for guiding prenatal care. Current methods, like using the last menstrual period, can be unreliable due to imprecise recall and symptoms such as early pregnancy bleeding that may be mistaken for a period [1–3]. Although fetal ultrasound is the most precise method, it is limited by timing and resource availability [4–8] and is most effective when performed before 20 weeks [9–11]. Ultrasound also requires advanced equipment and skilled personnel [6, 8, 12–14], highlighting the need for a more accessible and precise GA dating method, especially in diverse socioeconomic contexts.

Advances in omics technology offer new ways to explore the dynamic changes in pregnancy, capturing shifts in the maternal transcriptome, proteome, and metabolome [15, 16]. The metabolome, reflecting biochemical reactions, particularly responds to metabolic changes during pregnancy [17, 18]. Investigation of longitudinal maternal metabolomic alternations over the course of pregnancy has the potential to be a highly informative approach for mechanistic investigation and a breakthrough tool for GA dating. This approach has recently attracted more attention [18–20] but has relied mostly on maternal blood samples [18, 21–23]. The use of maternal urine for GA dating and metabolic profiling has yet to be comprehensively explored, and it may provide a cost-effective and non-invasive method that could be easily translated into clinical settings. If found to be useful, it would transform prenatal care, especially in under-resourced regions. At present, the cost of implementing and maintaining liquid chromatography–mass spectrometry (LC–MS)-based untargeted metabolomics far exceeds that of ultrasound. In the future, as specific metabolite biomarkers are identified and validated, the clinical application of metabolomics could shift toward more cost-effective approaches, such as targeted metabolomics methods or simple immunoassays based on these biomarkers could be developed. These methods require significantly less infrastructure and expertise than LC–MS, making them more accessible and affordable, particularly in under-resourced settings.

So far, research has focused on metabolic biomarkers for risks like preeclampsia and preterm birth (PTB) [24–31]. However, metabolomic profiling throughout pregnancy could improve understanding of maternal metabolic changes, allowing for better risk stratification and insight into the pregnancy process [18, 32, 33]. In this study, we analyzed longitudinal urine samples from 36 pregnant women, identifying numerous metabolites linked to pregnancy progression. We examined shifts in maternal

Received: November 11, 2024. **Revised:** January 9, 2025. **Accepted:** January 29, 2025

metabolic pathways and developed a model to predict GA, identifying individualized metabolic alterations throughout pregnancy.

Results

The SMART Diaphragm pregnancy cohort

This observational study aimed to determine if the urine metabolome could identify metabolic changes and predict GA. We analyzed urine samples from 36 pregnant women recruited in San Francisco as part of the SMART Diaphragm (SMART-D) study (Fig. 1a). SMART-D developed a vaginal device to detect cervical changes for early PTB risk prediction. Samples, including urine and cervicovaginal swabs, were collected longitudinally during pregnancy and postpartum. For this study, at least one urine sample was collected per trimester from each participant, resulting in 3–13 samples per participant (median: 10). Participants in the SMART-D study represented diverse backgrounds. The 36 participants were of four races (Asian, Black, Pacific Islander, and White), aged 21–39 years. Pre-pregnancy BMI ranged from 19.5 to 57.2, and parity ranged from 1 to 9 (Fig. 1b; Fig. S1a and b). Detailed characteristics are in Table S1. Data is also shown at: http://47.100.52.12:3838/smartd-shiny/.

The urine metabolome accurately reflects metabolic alterations during pregnancy

Untargeted metabolomics was performed, identifying 20 314 chemical signals (peaks; Fig. 1c). After removing 44 outlier samples, 302 samples remained for analysis (Fig. S1c). The batch effect has been largely mitigated, as indicated by the PCA score plot (Fig. S2), confirming high data quality. The SMART-D study's frequent sampling enabled detailed tracking of metabolome changes throughout pregnancy (Fig. 1d).

PCA of peaks (QC RSD < 30%) showed a clear separation between early and late GA samples, with postpartum samples closely resembling early GA samples (Fig. 1e). Most participants followed this overall pattern (Fig. S3). Significance analysis for microarrays (SAM) and linear regression identified 14.87% of peaks as significantly altered during pregnancy (Fig. 1f). Unsupervised k-means clustering revealed three clusters correlated with GA: cluster 1 (10–26 weeks), cluster 2 (26–32 weeks), and cluster 3 (32–42 weeks; Fig. 1g; Fig. S4). Consistent with PCA, postpartum samples mostly fell into cluster 1. These findings confirm that the urine metabolome reliably reflects metabolic shifts during pregnancy.

Alterations of functional metabolic network and pathways during pregnancy

An important strength of this study is the high-density sampling, providing detailed insights into metabolic regulation at each pregnancy stage. Samples were assigned to 14 GA ranges based on sampling times, with each range including at least ten subjects and samples to ensure robust analysis (Fig. 2a). Altered peaks were identified using the Wilcoxon signed-rank test [false discovery rate (FDR)-adjusted $P < .05$] compared to the baseline (Fig. 2b). Notably, 84.83% of altered peaks remained significant across all subsequent GA ranges, indicating a consistent pattern of metabolic changes throughout pregnancy (Fig. S5).

The number of altered peaks significantly increased from early to late pregnancy (Fig. 2b), aligning with the PCA and k-means clustering results. After childbirth, the number of altered peaks dramatically decreased compared to baseline. Based on the number of altered metabolic signatures, pregnancy metabolic signals were classified into four distinct periods: 10–18 weeks, 18–26 weeks, 26–34 weeks, and 34–42 weeks. These findings correspond with the clustering patterns observed (Fig. 1d).

To investigate changes in specific metabolic networks across GA ranges, altered peaks were analyzed using PIUMet [34], identifying a network of altered metabolites for each range. All annotated metabolites from PIUMet were then used to build a cross-sectional correlation network (Fig. 2c). The network included 160 nodes (metabolites) and 1148 edges (correlations), with 80.4% of annotated metabolites represented, suggesting dense interactions and a coordinated regulatory network for metabolic changes during pregnancy (Fig. 1d).

Using community analysis based on edge betweenness centrality [35, 36] revealed 20 clusters with a modularity of 0.30. Seven clusters (> 5 modes) were selected for further analysis (Fig. 2c; Fig. S6a). These clusters retained 76.25% of nodes and 96.95% of edges from the original network, indicating that they captured most of the correlations. These clusters likely represent physiologically related and correlated metabolites during pregnancy.

We analyzed alterations in the seven clusters during pregnancy by cluster and peak intensity (Fig. S6b and c). Only clusters 2 and 3 showed consistent changes at both levels. Cluster 2, the largest with 75 nodes and 963 edges, mainly includes lipids and lipid-like molecules (51/75, Fig. 2d), indicating a lipid-related regulatory network during pregnancy. The top pathways for cluster 2 metabolites were steroid hormone biosynthesis, ovarian steroidogenesis, cortisol synthesis, aldosterone synthesis, prolactin signaling, aldosterone-regulated sodium reabsorption, and bile secretion (Fig. 2d). Metabolite levels in cluster 2 increased throughout pregnancy, with rapid increases at weeks 18 and 26, aligning with periods defined in Figs 1d and 2b. Cluster 3, with five metabolites (3-methylguanine, 7-methylguanine, L-phenylalanine, asymmetric dimethylarginine, and (S)-3-hydroxy-N-methylcoclaurine), displayed similar trends. While no pathway mapped to more than one metabolite, four of five metabolites related to amino acid modification, suggesting cluster 3's involvement in amino acid metabolism (Fig. S6b and c).

Pathway enrichment analysis was conducted with PIUMet for each GA range to investigate pregnancy-related metabolic pathways further. Thirteen pathways showed enrichment in at least one GA range, with most increasing during pregnancy (FDR-adjusted $P < .05$, overlap ≥3; Fig. 2f). Six pathways were consistent at both the metabolite and pathway levels (Fig. 2g and h). Five of these six pathways overlapped with those in the regulated network of cluster 2.

Prediction of gestational age using the urine metabolome

Next, we explored whether the urine metabolome could estimate GA, which could improve prenatal and neonatal care in cases of uncertain dating. Urine samples were divided into training (16 subjects, 125 samples) and validation (20 subjects, 156 samples) datasets (Fig. S1b). Demographics and birth characteristics did not significantly differ between these datasets ($P > .05$, Table S1).

A random forest (RF) prediction model was built using 28 selected peaks identified through the Boruta algorithm and peak shape filtering (Table S3; Fig. S7a). The training dataset was utilized as the internal dataset to validate prediction accuracy using the bootstrap method. The root mean squared error (RMSE) between actual and predicted GA was found to be 2.35 weeks, and adjusted R^2 was 0.86 (Pearson correlation $r = 0.93$; $P < 2.2 \times 10^{-6}$;

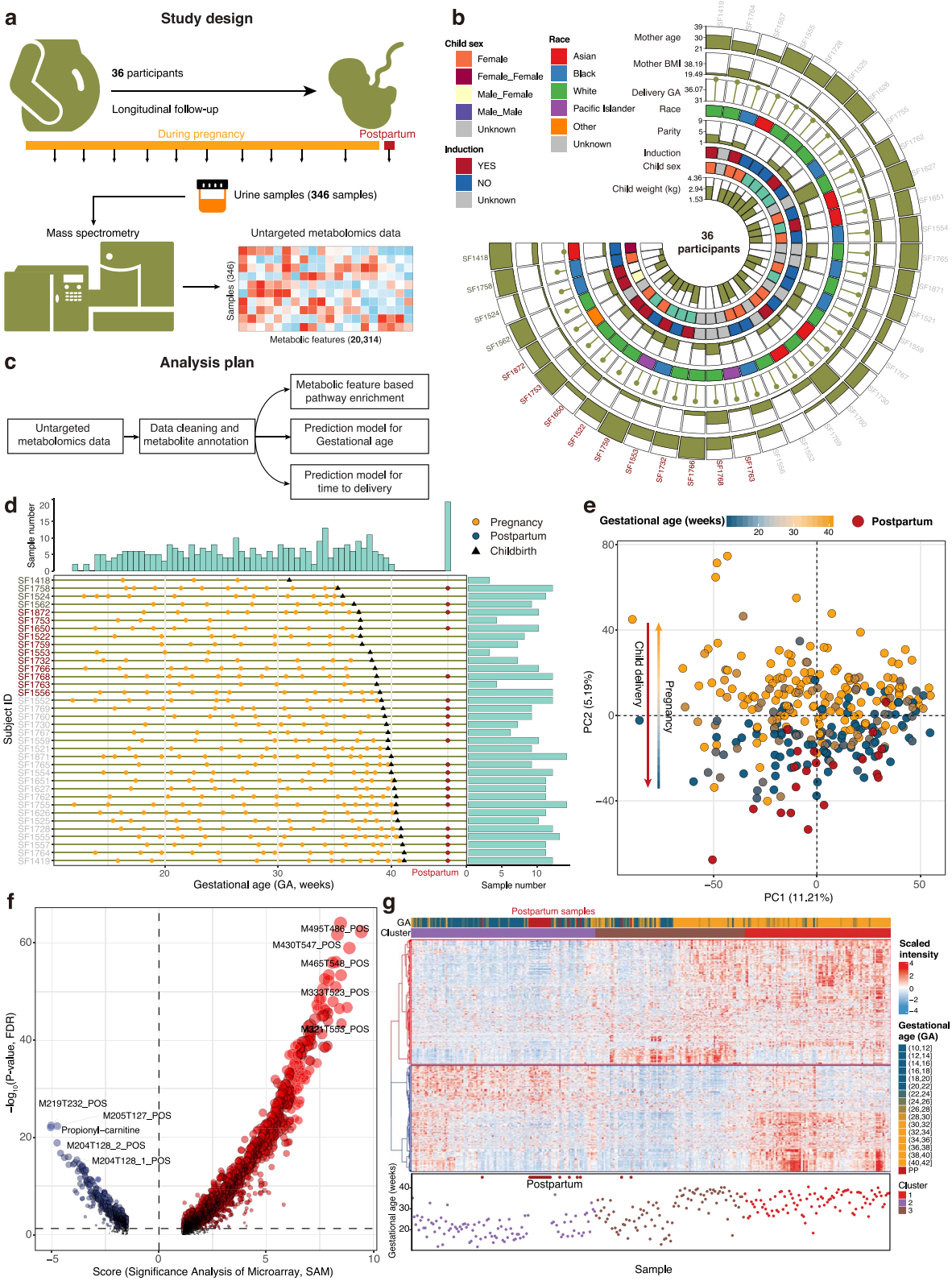

Figure 1. Study overview. (a) Study design. (b) Demographics of 36 participants. (c) Analysis plan. (d) Sampling time points per participant. (e) PCA of urine samples by GA. (f) Volcano plot of altered peaks during pregnancy. (g) K-means clustering of 3020 altered peaks into three groups.

Fig. S7b). External validation yielded an RMSE of 2.66 weeks and adjusted R^2 of 0.79 ($r = 0.89$; $P < 2.2 \times 10^{-6}$; Fig. S7c), indicating the model was not overfitting. Overall, our results demonstrated that the urine metabolome may be useful for accurately predicting GA.

The impact of patient demographics on prediction accuracy was also assessed. Maternal BMI, age, parity, and race were included with 28 peaks to construct a prediction model. The RMSE of this model was 2.70, and the adjusted R^2 was 0.76, which demonstrated no significant differences compared to the prediction model utilizing 28 peaks. The inclusion of subject demographics minimally improved prediction accuracy.

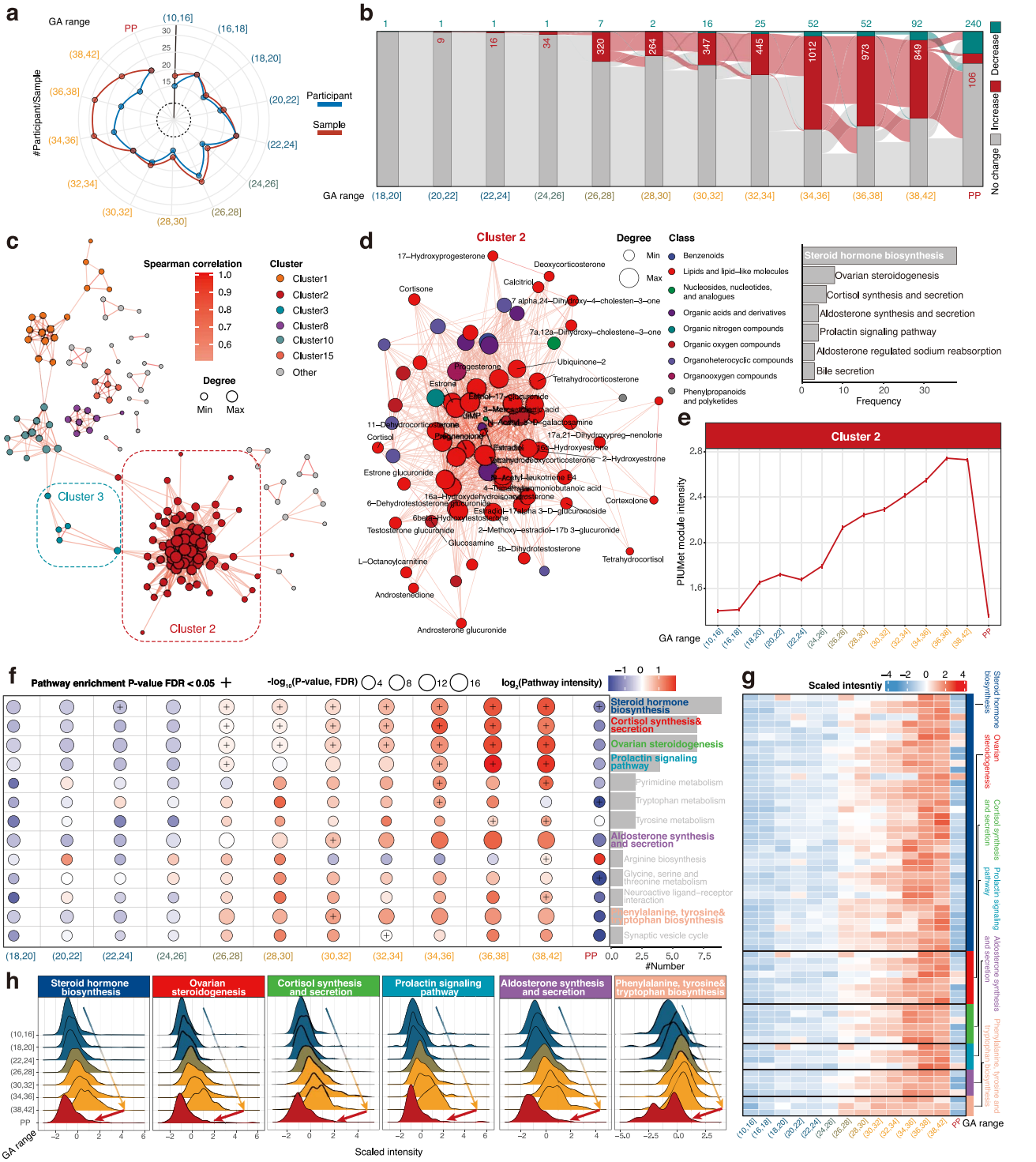

Figure 2. Dynamic changes in the urine metabolome during pregnancy. (a) Participant and sample counts per GA range. (b) Altered peaks in each GA range versus baseline. (c) Correlation network using PIUMet-annotated peaks. (d) Cluster 2 identified via community analysis shows consistent changes at cluster and metabolite levels; pathway frequencies per metabolite on the right. (e) Cluster 2 changes during pregnancy. (f) Altered pathways per GA range. (g) Heatmap of 6 metabolic pathway changes at the metabolite level. (h) Ridgeline plot of 6 metabolic pathway changes at the pathway level.

Prediction of gestational age at the individual level

Our study demonstrated that the pregnancy urine metabolome, using 28 peaks, can accurately predict GA. Peaks were annotated through an in-house MS2 pipeline [37–39], with 875 of 20 314 peaks annotated at level 1 or 2, though only 5 of the final 28 peaks were annotated (Table S3). Using these 875 metabolites, we selected 32 for prediction, refining to 21 biomarkers after excluding those with poor peak shapes and MS^2 matches (Figs S8 and S9). Most biomarkers were lipids and lipid-like molecules (Fig. 3a, Table S4) [40], aligning with maternal plasma findings [18, 41–43].

Most biomarkers ranked highly in the prediction model (Fig. 3a; Fig. S10). The 21 metabolite biomarkers achieved similar accuracy to the peak model, with adjusted R^2 of 0.81 ($r = 0.90$, $P < 2.2 \times 10^{-6}$)

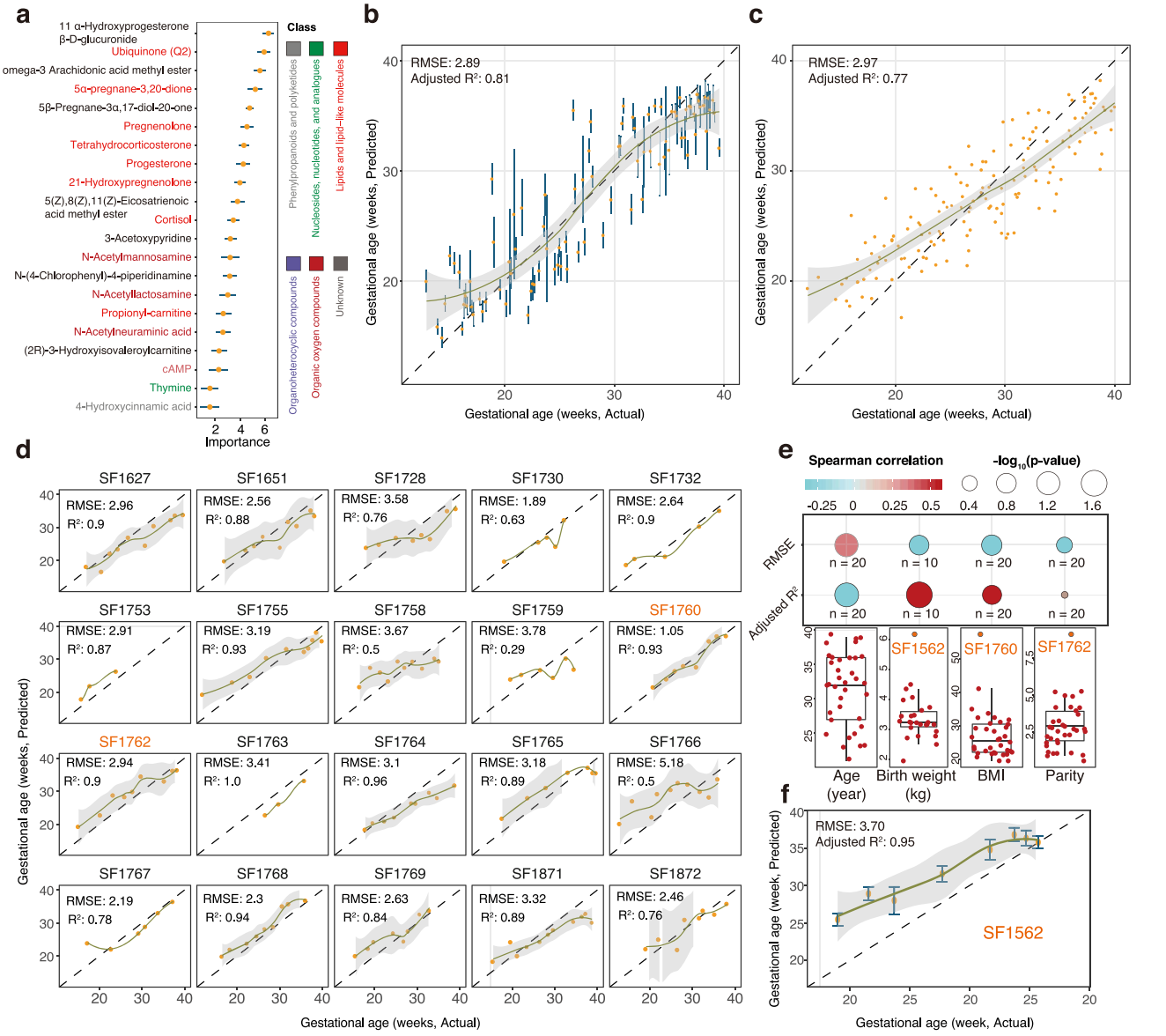

Figure 3. Urine metabolomics predicts GA at the individual level. (a) Twenty-one biomarkers selected. (b and c) GA prediction aligns closely with clinical values in internal (b) and external (c) validation datasets. (d) Individual prediction accuracy. (e) Continuous characteristics do not affect accuracy. (f) Outlier SF1562 in birth weight achieves good accuracy.

for internal validation and 0.77 ($r = 0.87$, $P < 2.2 \times 10^{-6}$) for external validation datasets (Fig. 3b and c). The RMSE was 2.89 weeks for internal and 2.97 weeks for external validation (Fig. 3b and c). A 1000-time permutation test confirmed no overfitting (Fig. S11). Notably, model performance improved over pregnancy, with RMSE decreasing from the first to the third trimester for both training (4.71 in T1, 2.81 in T2, 2.82 in T3) and validation datasets (7.30 in T1, 3.14 in T2, 2.81 in T3; Fig. 4c and d). There was also no significant difference in accuracy between the metabolite and peak models, particularly in the validation dataset (RMSE = 2.97 *versus* 2.66 weeks, adjusted $R^2 = 0.77$ *versus* 0.79).

These results indicate that urine metabolites can effectively predict GA and have promising clinical applications. When applied to individual participants in the external validation dataset, 16 out of 20 achieved an adjusted R^2 >0.75 (Fig. 3d; Fig. S12, Table S5), demonstrating the robustness of our model for individual predictions. Our cohort, which includes women with diverse demographic and clinical characteristics (Fig. S1a and b), suggests the model's utility across varied backgrounds.

We then assessed the impact of individual characteristics on prediction accuracy, calculating correlations between RMSE/adjusted R^2 and continuous variables. Surprisingly, continuous factors showed no significant correlation with prediction accuracy (all $r < 0.5$, all $P > .05$; Fig. 3e). Notably, three participants were outliers for birth weight, BMI, and parity. Participant S1760 had a BMI of 57.23 (mean: 27.09, $P < .001$) with high prediction accuracy (RMSE = 1.05, adjusted $R^2 = 0.93$; Fig. 3d). Participant S1762, with parity of nine (mean: 2.92, $P < .001$), also achieved good accuracy (RMSE = 2.94, adjusted $R^2 = 0.90$; Fig. 3d). For S1562, with a birth weight of 6.185 kg (mean: 3.397 kg, $P < .001$), internal validation accuracy was similarly high (RMSE = 3.70, adjusted $R^2 = 0.95$; Fig. 3f).

We also examined whether categorical characteristics influenced prediction accuracy. Results indicated that prediction accuracy was unaffected by these factors (Fig. S13, analysis of variance test, all $P > .05$). Overall, these findings demonstrate that the GA prediction model based on metabolite biomarkers is highly robust and adaptable to individual diversity.

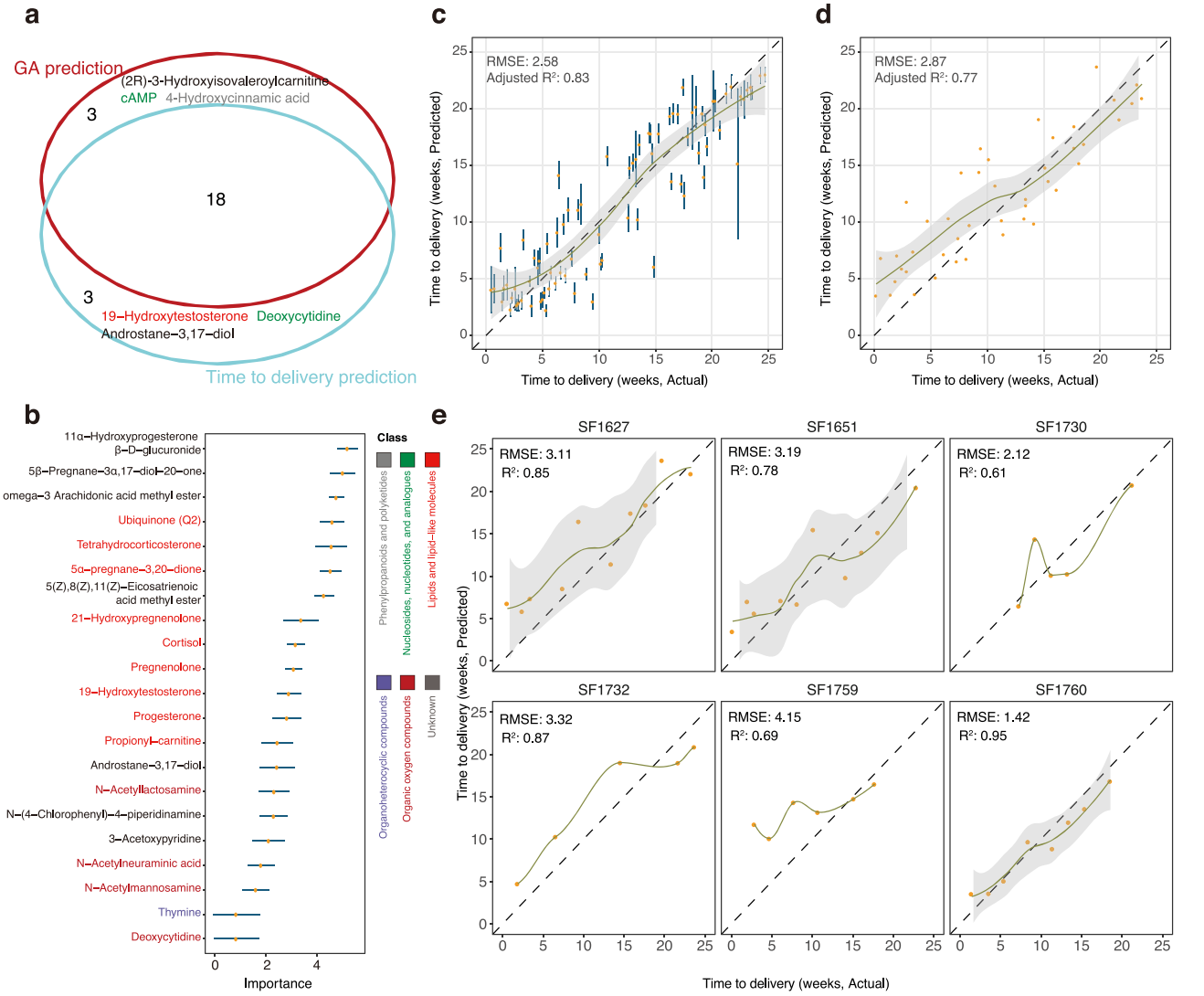

Figure 4. Urine metabolome predicts individual time-to-delivery. (a) Overlap of metabolites between GA and time-to-delivery models. (b) Twenty-one biomarkers for time-to-delivery model. (c and d) Predicted time-to-delivery closely matches actual values in internal (c) and external (d) validations. (e) Individual prediction accuracy.

Prediction of time to delivery using the urine metabolome

We next evaluated whether the urine metabolome could predict time-to-delivery, defined as the difference between GA at sample collection and GA at delivery, independent of ultrasound estimates. Participants with scheduled Cesarean sections were excluded, leaving 20 participants (Table S2). The model included 21 metabolites, 18 of which overlapped with those in the GA prediction model (Fig. 4a and b; Table S4). Predicted values aligned well with actual values in both the training (RMSE = 2.58 weeks; adjusted $R^2 = 0.83$; $r = 0.94$, $P < 2.2 \times 10^{-6}$; Fig. 4c) and validation datasets (RMSE = 2.87; adjusted $R^2 = 0.77$; $r = 0.88$, $P = 4.91 \times 10^{-15}$; Fig. 4d). A permutation test confirmed no overfitting (Fig. S14). Prediction accuracy was also unaffected by patient demographics, similar to the GA model (Fig. S15a). These findings show that the time-to-delivery model is robust and effective across diverse individual characteristics.

Altered metabolic signatures during pregnancy

We also examined the biological function of the 24 metabolite markers. Most of the markers (9 of 24; 8 are unknown) were lipids and lipid-like molecules (primarily hormones, Table S4; Fig. S15b), aligning with earlier findings at the peak level.

To capture shifting metabolic signatures, hierarchical and fuzzy c-mean clustering grouped the 24 markers into two clusters with contrasting regulation patterns (Fig. 5a–c). The first group showed downregulation during pregnancy, returning to normal postpartum (Fig. S16a), while the second group increased with pregnancy and normalized postpartum (Fig. S16b). This second group was enriched in pathways related to glucocorticoid and mineralocorticoid biosynthesis, growth hormones, and lipid metabolism. Given progesterone's clinical relevance in PTB treatment [44–47], other similarly regulated steroids may serve as diagnostic or therapeutic targets.

Correlation analysis across GA periods revealed significant metabolomic shifts as the pregnancy progressed (Fig. 5d). Early pregnancy showed a positive correlation between metabolite intensity and GA, shifting to a negative correlation in later stages, indicating that urine metabolome alterations may help predict delivery timing.

Further analysis showed positive correlations among many markers and delivery-related factors, such as maternal BMI and birth weight, suggesting co-regulated metabolic pathways,

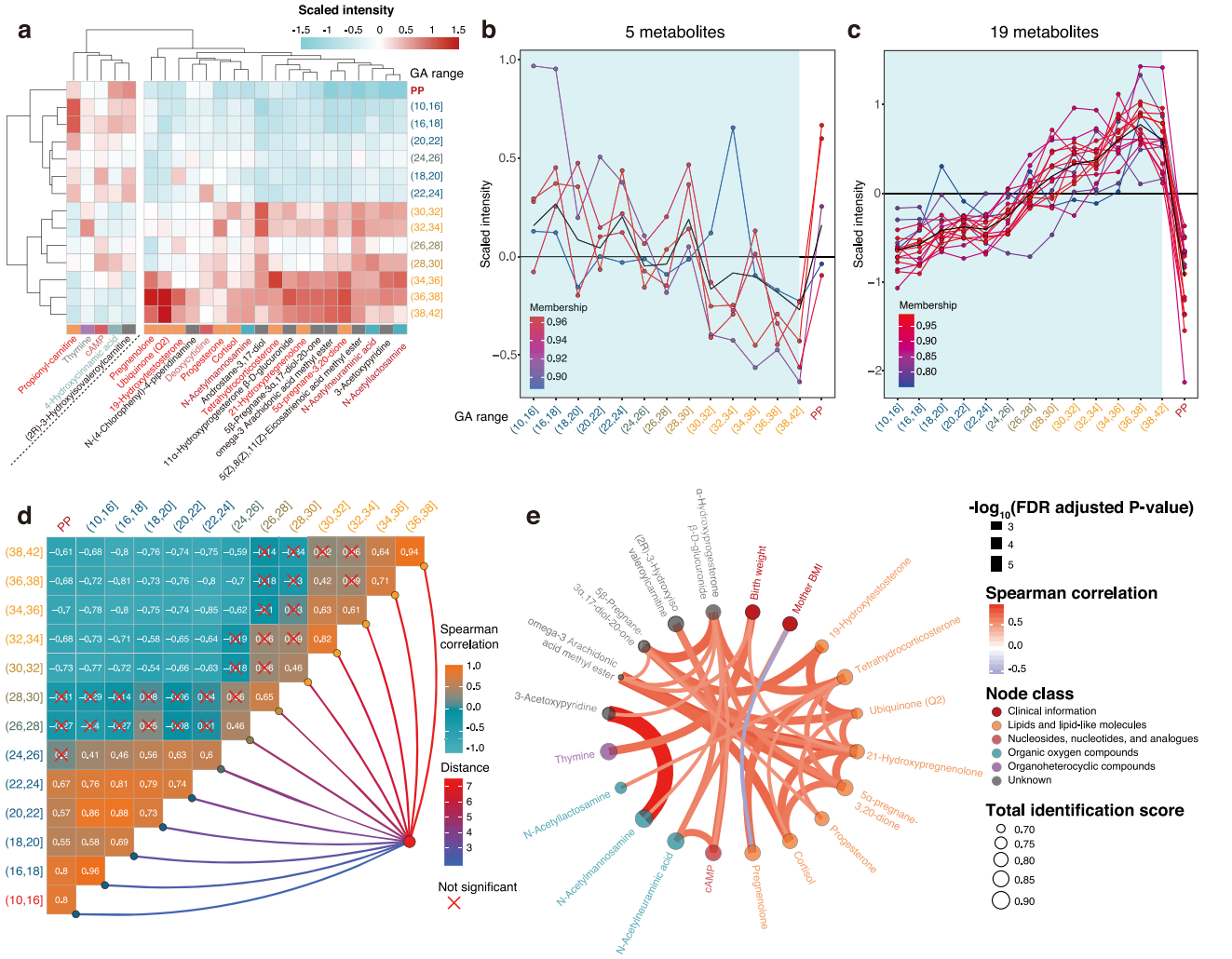

Figure 5. Integrative analysis of GA markers. (a) Marker clustering. (b and c) Biomarker clustering: one group shows downregulation returning to normal postpartum (b); another shows upregulation, then downregulation postpartum (c). (d) Correlation of metabolome changes across GA and proximity to postpartum. (e) Correlations between markers.

with the exception of a negative correlation between BMI and pregnenolone (Fig. 5e). This aligns with studies linking obesity to higher PTB risk [48–50], suggesting that pregnenolone levels might aid in GA prediction and preterm risk assessment. Although BMI showed no significant correlation with most lipid biomarkers (except BMI-pregnenolone, FDR adjusted $P < .05$), a non-significant trend of negative correlation with other lipids was observed (Fig. S17a).

Discussion

Accurate GA estimation is essential for preventive prenatal care and timely interventions as maternal and fetal needs change throughout pregnancy [18, 51]. While metabolic changes in pregnancy have been extensively studied using blood samples [16, 18, 52, 53], the comprehensive dynamics of the pregnancy urine metabolome remain less explored. In this study, we used comprehensive metabolic profiling of urine samples to better understand prenatal and postnatal metabolic changes in maternal urine. We developed models to predict GA and time-to-delivery with strong predictive accuracy at both cohort and individual levels (training: adjusted $R^2 = 0.81$, RMSE = 2.89; validation: $R^2 = 0.77$, RMSE = 2.97). The GA model tended to overestimate in early pregnancy and underestimate in later stages, possibly due to diverse biological processes that require further study in larger cohorts. Overall, our findings demonstrate the potential of the urine metabolome for accurate GA estimation and time-to-delivery prediction.

Pregnenolone, progesterone, and corticoids were all upregulated in the glucocorticoid pathways during pregnancy, and related metabolites used in the time-to-delivery prediction model were enriched for glucocorticoid and CMP-N-acetylneuraminate biosynthesis pathways. These hormones have been reported to play key roles in pregnancy regulation [45–47]. For instance, progesterone has been approved for the treatment of amenorrhea, metrorrhagia, and infertility [54–56]. In our previous study of maternal plasma collected in an independent cohort, we also identified tetrahydrodeoxycorticosterone, estriol glucuronide, and progesterone as markers for GA estimation [18]. Other identified derivatives in the same steroid hormone group of estrogens and progesterone derivatives, as well as uncharacterized steroid-like compounds discovered in this study, may also play roles in pregnancy, although their functions remain unclear. Furthermore, N-acetylmannosamine and N-acetylneuraminate were both significantly upregulated in the CMP-N-acetylneuraminate biosynthesis pathway, although the impact of these signaling molecules on pregnancy-related processes remains to be explored.

As a proof of principle, our results show that urine metabolomic profiles can be used to track gestation throughout pregnancy. By applying an RF model, we successfully predicted GA based on 21 urine metabolites (Fig. 3a), including diverse glucocorticoids, lipids, glucuronide, and amino acid derivatives, indicating comprehensive regulation of glucocorticoid biosynthesis and CMP-N-acetylneuraminate biosynthesis by pregnancy.

Compared to previous research [57, 58], which employed targeted or restricted metabolomic approaches, our study utilizes untargeted LC–MS to capture a broader spectrum of metabolic features. By analyzing longitudinal samples across the entire pregnancy (11–40 weeks), we identified key metabolic shifts and constructed a GA prediction model. While prior studies demonstrated the feasibility of urinary metabolomics for GA estimation, our study advances this field by offering enhanced predictive performance and a more comprehensive understanding of pregnancy-associated metabolic changes.

While our study provides valuable insights into the potential of urine metabolomics for GA prediction, our study still has several limitations that need to be addressed in future studies. First, the cohort size is relatively small (36 participants), which limits the generalizability of the findings. Future studies should aim to validate these findings in larger and more diverse cohorts to ensure broader applicability and to assess the robustness of the model across different populations and settings. Additionally, To mitigate overfitting risks, we used the Boruta algorithm for robust feature selection and employed cross-validation within the training dataset. However, the small cohort size and high-dimensional nature of metabolomics data could still pose overfitting risks, warranting further validation in larger, independent cohorts.

Second, while our analysis identified significant metabolites and pathways associated with GA, and we took additional steps to enhance the quality of selected biomarkers by excluding metabolites with poor peak shapes or weak MS^2 matches, the biological roles of some unannotated metabolites remain unclear. This underscores the need for further research to characterize these unknown features and explore their potential contributions to pregnancy-related metabolic changes in urine samples. Future studies could leverage advanced algorithms and emerging methodologies to improve the characterization and annotation of these unannotated metabolites. Additionally, although only a small proportion of peaks were annotated, the metabolites selected for the predictive model underwent rigorous statistical validation using the Boruta algorithm and cross-validation to minimize overfitting and maximize reproducibility. We also excluded metabolites with poor peak shapes or weak MS^2 matches to enhance the quality of the selected biomarkers further.

Third, while we controlled for key demographic and clinical factors such as BMI and parity, other potential confounders, including dietary intake, medication use, and environmental exposures, were not accounted for due to the lack of available data. These factors may influence metabolomic profiles and could contribute to variability in our findings. Future studies should aim to incorporate detailed dietary, medication, and environmental exposure data to comprehensively assess their effects on metabolomic profiles and improve the robustness of predictive models.

Fourth, although normalization was applied to minimize variability, residual batch effects cannot be completely excluded, particularly given the complexity of untargeted metabolomics datasets. Advanced techniques may further reduce batch-related noise in future studies.

Fifth, while the FDR-adjusted threshold minimizes false positives, it may still overlook subtle but biologically meaningful changes, particularly in high-dimensional datasets where signal-to-noise ratios can vary.

Finally, different omics data provide unique insights into the human body, each capturing distinct aspects of biological processes. The findings presented here are based solely on metabolomics data. In the future, integrating metabolomics data with other omics layers, such as proteomics and genomics, could significantly enhance the accuracy and robustness of GA estimation. Indeed, several studies have demonstrated that combining metabolomics with other omics data in blood samples improves GA prediction accuracy [33, 59]. We anticipate that integrating multi-omics data from urine and other biological samples will not only enhance the precision of GA prediction but also provide a more comprehensive understanding of the molecular mechanisms underlying pregnancy progression.

The characterized alterations in the maternal urine metabolome showed a strong correlation with GA and pregnancy progression. Accurate and convenient GA determination and time-to-delivery prediction can enhance fetal development monitoring and support timely interventions to improve maternal and infant health. Monitoring maternal metabolic changes and their association with GA could offer deeper insights into fetal development regulation and pregnancy disorders. The non-invasive and accessible nature of urine metabolomics makes it a valuable tool for GA assessment in diverse clinical settings, especially in resource-limited areas with restricted access to early prenatal care.

Methods

Participant enrolment and urine sample collection

A total of 346 urine samples were collected from 36 ethnically diverse women throughout pregnancy (11.8–40.7 weeks) and postpartum (Table S1). The information for 'duction', 'child sex', and 'child weight' is missing for 10 participants in our cohort due to incomplete data collection (Table S1). Samples were collected longitudinally in two batches (Table S6), with GA dating based on American Congress of Obstetricians and Gynecologists guidelines. Urine samples were collected as random spot urine samples at various time points during pregnancy and postpartum. No 24-hour urine collections were performed.

Chemical material and internal standard preparation

MS-grade solvents (water, methanol, acetonitrile) were from Fisher Scientific. MS-grade acetic acid and analytical-grade internal standards were from Sigma Aldrich. The internal standard mixture (acetyl-d3-carnitine, phenylalanine-3,3-d2, tiapride, trazodone, reserpine, phytosphingosine, and chlorpromazine) was diluted 1:50 with a 3:1 acetonitrile-water solution for HILIC and with water for RPLC.

Urine sample preparation

Thawed urine samples were centrifuged at 17 000 rcf for 10 minutes; 250 μL of supernatant was diluted with 750 μL of internal standard. After a 10-second vortex and another 10-minute centrifuge at 17 000 rpm (4°C), the supernatant was used for LC–MS. A pooled QC sample was injected every 10 samples to ensure consistent retention time and signal intensity. All samples were

randomized during sample preparation and data acquisition to minimize bias introduced by batch effects or systematic trends.

Liquid chromatography–mass spectrometry data acquisition

A Hypersil GOLD HPLC and guard columns (Thermo Scientific, San Jose, CA) were used for RPLC. The mobile phases were 0.06% acetic acid in water (A) and methanol with 0.06% acetic acid (B), with a flow rate of 0.25 mL/min and backpressure of 120–160 bar at 99% phase A. A linear gradient from 1% to 80% phase B was applied >9–10 minutes. The column was heated to 60°C, and the sample injection volume was 5 μL.

HILIC experiments were performed using a ZIC-HILIC column (Merck Millipore) and mobile phase solvents consisting of 10 mM ammonium acetate in 50/50 acetonitrile/water (A) and 10 mM ammonium acetate in 95/5 acetonitrile/water (B). Metabolites were eluted from the columns at 0.5 ml/min using a 1–50% phase A gradient >15 min.

The Thermo Q Exactive Hybrid Quadrupole-Orbitrap Plus and Q Exactive mass spectrometers (Xcalibur, Thermo Scientific, San Jose, CA, USA) were operated in full MS-scan mode for data acquisition, covering an m/z range of 50 to 1000. For MS^1 acquisition, the instruments were set with a scan rate of ∼1.5 Hz, a resolution of 10 000 (at m/z 127), an injection time of 50 ms, and an automatic gain control (AGC) target of 3×10^6. MS/MS spectra for the QC sample were acquired using the top 10 parent ions, fragmented at normalized collision energies (NCE) of 25 and 50, with an injection time of 100 ms and an AGC target of 1×10^5.

Data processing and cleaning

MS raw data were converted to .mzXML (MS^1) and .mgf (MS^2) formats using ProteoWizard (Table S7). Peak detection and alignment were done via an in-house pipeline [37], producing an MS^1 peak table. Across the dataset, an average of 12.5% of data points per feature were missing prior to imputation. Features with >20% missing values in QC samples were excluded from the analysis to minimize the potential for bias. We also excluded samples with >50% missing values (outlier samples) and imputed remaining gaps using the k-nearest neighbors algorithm (KNN). We selected KNN imputation as it is a widely used method in metabolomics studies due to its ability to estimate missing values based on the similarity of observed features [60]. Outlier samples were defined as the samples with >50% missing values. Outlier samples were removed to prevent potential biases in downstream statistical analyses and machine learning modeling. These samples exhibited aberrant metabolomic profiles likely caused by technical errors, such as incomplete sample preparation, instrument fluctuations, or contamination. Peak intensity was normalized by mean, with batch mean ratios applied for data integration. To account for variability in urine concentration, the mean normalization was applied to the dataset. This approach was selected due to its simplicity and effectiveness in controlling for systematic biases across samples. Although more specific methods, such as probabilistic quotient normalization (PQN), creatinine adjustment, or specific gravity correction, are available, we chose the mean normalization to maintain consistency with prior studies and ensure robust analysis across a diverse cohort [18].

General statistical analysis and data visualization

Most statistical analysis and data visualization were conducted in R (version 3.6.0, Table S8). Before analysis, data were log10 transformed and auto-scaled. Categorical data are reported as counts and percentages, while continuous variables are presented as the mean ± standard deviation or standard error of the mean. Due to the right-skewed distribution of most peaks, nonparametric methods were used for statistical tests, with all *P*-values adjusted using the FDR. The FDR-adjusted p-value threshold of 0.05 was selected to balance sensitivity and specificity in identifying significant features while controlling for the high-dimensional nature of metabolomics data. This threshold is widely accepted in metabolomics and omics studies as a rigorous standard for multiple testing correction.

SAM test and linear regression model to detect overall altered peaks during pregnancy

To identify peaks that significantly changed with GA, we applied a SAM and a linear regression model [18, 61]. SAM uses permutations of repeated measurements to estimate the FDR for peaks exceeding an adjustable threshold. The linear regression model was built using the R 'lm' function, adjusting for acquisition batch, BMI, maternal age, parity, and race. Peaks with an FDR-adjusted $P < .05$ were considered significant.

K means consensus-clustering

Unsupervised K-means consensus clustering was conducted using the R packages CancerSubtypes and ConsensusClusterPlus. Sample clusters were identified with K-means clustering, Euclidean distance, and 1000 resampling repetitions across 2 to 6 clusters. The empirical cumulative distribution function plot suggested 2 or 3 clusters as optimal for all urine samples. Consensus matrix heatmaps also indicated that 2, 3, and 4 clusters showed good separation. To determine the optimal cluster number, we extracted silhouette scores using the silhouette_SimilarityMatrix function. Comparing k = 2, 3, and 4, we found that k = 3 provided the highest clustering stability (Fig. S4).

PIUMet analysis

PIUMet, a network-based tool, links peaks to potential metabolites and related dysregulated molecular mechanisms, effectively converting peak data into network information [34]. For each GA range, altered peaks were saved as .txt files and uploaded to the PIUMet website. Results from PIUMet were then processed through an in-house pipeline, where annotation results across GA ranges were combined. Peaks appearing in fewer than two GA ranges were removed, and mean values of matched peaks were used as quantitative values for each metabolite.

Correlation network and community analysis

For the combined dataset of metabolites and clinical variables, correlations between variables were calculated, and only pairs with an absolute correlation >0.5 and FDR-adjusted $P < 0.05$ were used to construct correlation networks. Community analysis was performed with edge betweenness-based detection (Girvan–Newman method). This method iteratively removes edges with the highest edge betweenness, which likely connect separate modules until individual nodes remain. The result is a dendrogram, with leaves as individual nodes and the root as the whole network.

Modularity analysis was used to identify communities within the network, maximizing modularity at each iteration to identify statistically significant structures (Fig. S7a). Only clusters with at least three nodes were retained for further analysis.

Kyoto Encyclopedia of Genes and Genomes pathway enrichment analysis

Pathway enrichment analysis was conducted using the KEGG database, a widely used resource in metabolomics, which initially contains 275 pathways divided into metabolic and disease pathways based on the 'Class' information. Enrichment analysis was performed using a hypergeometric distribution test, with *P*-values adjusted by the FDR method and a significance cutoff of .05.

Metabolite annotation

The metabolite annotation was performed using the metID package [38]. For the metabolite annotated using the in-house database [39, 62], the annotations are level 1 according to MSI [63]. For metabolites annotated using the public databases, the annotation is level 2, according to MSI [63].

The random forest prediction model

Feature selection. The Boruta algorithm was used to identify biomarkers by creating shadow features through shuffling and then comparing them to real features via RF classification, repeated 100 times for robustness. Selected features served as potential biomarkers for the RF model.

Parameter optimization. Default settings were used except for ntree (trees) and mtry (variables per split) in the RF model, optimized in the training set by minimizing MSE.

GA prediction model. Samples from batch 1 (16 subjects, 125 samples) were used for training, and batch 2 (20 subjects, 156 samples) for validation. Feature selection was performed on the training dataset, followed by the construction of the RF model. A linear regression model was then applied between predicted and actual GA to correct predictions (Fig. S17b). This two-part model was validated on external samples, with RMSE and adjusted R^2 used to assess accuracy.

1000 bootstraps resampled 63% of training data, using 37% for validation; final GA predictions averaged per sample, calculating MSE and adjusted R^2.

Time-to-delivery prediction model. Calculated as weeks between sample and delivery dates, using the same approach as the GA model.

Permutation test

First, responses (GA or time to delivery) were randomly shuffled in the training and validation datasets. Potential biomarkers were selected, and RF parameters were optimized in the training dataset. An RF model was then built with selected features and applied to the validation dataset, yielding null RMSE and adjusted R^2 values. This process was repeated 1000 times to generate distributions of null RMSE and adjusted R^2 values. Using maximum likelihood estimation, these values were modeled with a Gamma distribution, and cumulative distribution functions were calculated to derive p-values for the actual RMSE and adjusted R^2.

Fuzzy c-means clustering

The fuzzy c-means clustering algorithm was used to classify metabolite biomarkers by GA. Samples were grouped into time ranges from 11 to 41 weeks in two-week increments, with postpartum samples assigned to a 'PP' group. For each time range, the mean intensity of each metabolite was calculated, creating a new dataset with 16 observations.

First, we optimized the parameter 'm' using Mfuzz and determined the optimal cluster number based on the within-cluster sum of squared errors. Using default parameters, fuzzy c-means clustering was performed, and only features with a membership score > 0.5 were retained. No smoothing was applied to the output results.

Key points

- This study applied Liquid chromatography–mass spectrometry-based untargeted metabolomics and metabolic peak-based pathway analysis to analyze longitudinal changes in maternal urine, highlighting significant alterations in glucocorticoids, lipids, and amino acid derivatives during pregnancy.
- A machine learning model based on urinary metabolites accurately predicts gestational age (GA), offering a non-invasive pregnancy dating method that is especially useful in resource-limited settings.
- The findings underscore the potential clinical utility of urine metabolomics in improving GA estimation and monitoring maternal metabolic health.
- The study provides a detailed, comprehensive characterization of the maternal urine metabolome, which could enhance prenatal care and maternal–fetal health management.

Acknowledgements

We thank the dedicated pregnant women who participated in this study. This work was supported by the UCSF California Preterm Birth Initiative.

Author contributions

L.R. and L.J.P. organized and contributed to pregnancy sample collection. L.L., S.C., X.S., L.J.P., L.R., and M.S. conceptualized the study and analysis plan. S.C., L.L., M.A., X.S., and H.Z. processed and analyzed samples, while X.S., S.C., and L.L. conducted data analysis. S.C., X.S., L.L., L.J.P., L.R., and M.S. drafted the manuscript, with all authors involved in reviewing and editing.

Supplementary data

Supplementary data is available at *Briefings in Bioinformatics* online.

Conflict of interest: M.P.S. is a cofounder, scientific advisor, and shareholder of Filtricine, Iollo, January AI, Marble Therapeutics, Next Thought AI, Personalis, Protos Biologics, Qbio, RTHM, and SensOmics. M.P.S. is a scientific advisor and equity holder of Abbratech, Applied Cognition, Enovone, M3 Helium, and Onza. M.P.S. is a scientific advisor and stock option holder of Jupiter Therapeutics, Mitrix, Neuvivo, Sigil Biosciences, WndrHLTH, and Yuvan Research. M.P.S. is a cofounder and stock option holder of Crosshair Therapeutics. M.P.S. is an investor and scientific advisor of R42 and Swaza. M.P.S. is an investor in Repair Biotechnologies. M.P.S. is a cofounder, shareholder, and director of Exposomics, Fodsel, and InVu Health. M.P.S. is a cofounder and equity holder of Mirvie, NiMo Therapeutics, and Orange Street Ventures. L.L. is a co-founder of NiMo. The remaining authors declare no competing interests.

Funding

None declared.

Data availability

All data are present in the paper or the Supplementary Materials.

Code availability

All code has been provided on GitHub (https://github.com/jaspershen-lab/smartd_project).

References

1. Alexander GR, Tompkins ME, Petersen DJ. *et al.* Discordance between LMP-based and clinically estimated gestational age: Implications for research, programs, and policy. *Public Health Rep* 1974;**1995**:395–402.
2. Wingate MS, Alexander GR, Buekens P. *et al.* Comparison of gestational age classifications: date of last menstrual period vs. clinical estimate. *Ann Epidemiol* 2007;**17**:425–30. https://doi.org/10.1016/j.annepidem.2007.01.035
3. Savitz DA, Terry JW, Dole N. *et al.* Comparison of pregnancy dating by last menstrual period, ultrasound scanning, and their combination. *Am J Obstet Gynecol* 2002;**187**:1660–6. https://doi.org/10.1067/mob.2002.127601
4. Papageorghiou AT, Kennedy SH, Salomon LJ. *et al.* International standards for early fetal size and pregnancy dating based on ultrasound measurement of crown-rump length in the first trimester of pregnancy. *Ultrasound Obstet Gynecol* 2014;**44**:641–8. https://doi.org/10.1002/uog.13448
5. McClure EM, Nathan RO, Saleem S. *et al.* First look: a cluster-randomized trial of ultrasound to improve pregnancy outcomes in low income country settings. *BMC Pregnancy Childbirth* 2014;**14**:73. https://doi.org/10.1186/1471-2393-14-73
6. Kim ET, Singh K, Moran A. *et al.* Obstetric ultrasound use in low and middle income countries: a narrative review. *Reprod Health* 2018;**15**:129. https://doi.org/10.1186/s12978-018-0571-y
7. Benson CB, Doubilet PM. Sonographic prediction of gestational age: accuracy of second- and third-trimester fetal measurements. *AJR Am J Roentgenol* 1991;**157**:1275–7. https://doi.org/10.2214/ajr.157.6.1950881
8. Jehan I, Zaidi S, Rizvi S. *et al.* Dating gestational age by last menstrual period, symphysis-fundal height, and ultrasound in urban Pakistan. *Int J Gynaecol Obstet* 2010;**110**:231–4. https://doi.org/10.1016/j.ijgo.2010.03.030
9. Kalish RB, Thaler HT, Chasen ST. *et al.* First- and second-trimester ultrasound assessment of gestational age. *Am J Obstet Gynecol* 2004;**191**:975–8. https://doi.org/10.1016/j.ajog.2004.06.053
10. Liang J, Zhou Z. Application of APACHE II scoring in ICU trauma patients. *Chin J Traumatol* 1998;**1**:58–60.
11. Sayers SM, Powers JR. An evaluation of three methods used to assess the gestational age of aboriginal neonates. *J Paediatr Child Health* 1992;**28**:312–7. https://doi.org/10.1111/j.1440-1754.1992.tb02675.x
12. Wier ML, Pearl M, Kharrazi M. Gestational age estimation on United States livebirth certificates: a historical overview. *Paediatr Perinat Epidemiol* 2007;**21**:4–12. https://doi.org/10.1111/j.1365-3016.2007.00856.x
13. Reuss ML, Hatch MC, Susser M. Early ultrasound dating of pregnancy: selection and measurement biases. *J Clin Epidemiol* 1995;**48**:667–74. https://doi.org/10.1016/0895-4356(94)00162-J
14. LaGrone LN, Sadasivam V, Kushner AL. *et al.* A review of training opportunities for ultrasonography in low and middle income countries. *Trop Med Int Health* 2012;**17**:808–19. https://doi.org/10.1111/j.1365-3156.2012.03014.x
15. Ullrich RL, Casarett GW. Interrelationship between the early inflammatory response and subsequent fibrosis after radiation exposure. *Radiat Res* 1977;**72**:107–21. https://doi.org/10.2307/3574561
16. Aghaeepour N, Lehallier B, Baca Q. *et al.* A proteomic clock of human pregnancy. *Am J Obstet Gynecol* 2018;**218**:347.e1–14. https://doi.org/10.1016/j.ajog.2017.12.208
17. Holmes E, Wilson ID, Nicholson JK. Metabolic phenotyping in health and disease. *Cell* 2008;**134**:714–7. https://doi.org/10.1016/j.cell.2008.08.026
18. Liang L, Rasmussen M-LH, Piening B. *et al.* Metabolic dynamics and prediction of gestational age and time to delivery in pregnant women. *Cell* 2020;**181**:1680–1692.e15. https://doi.org/10.1016/j.cell.2020.05.002
19. Wang Q, Würtz P, Auro K. *et al.* Metabolic profiling of pregnancy: cross-sectional and longitudinal evidence. *BMC Med* 2016;**14**:205. https://doi.org/10.1186/s12916-016-0733-0
20. Wang Q, Würtz P, Auro K. *et al.* Effects of hormonal contraception on systemic metabolism: cross-sectional and longitudinal evidence. *Int J Epidemiol* 2016;**45**:1445–57. https://doi.org/10.1093/ije/dyw147
21. León-Aguilar LF, Croyal M, Ferchaud-Roucher V. *et al.* Maternal obesity leads to long-term altered levels of plasma ceramides in the offspring as revealed by a longitudinal lipidomic study in children. *Int J Obes (Lond)* 2005;**2019**:1231–43.
22. Francis EC, Hinkle SN, Song Y. *et al.* Longitudinal maternal vitamin D status during pregnancy is associated with neonatal anthropometric measures. *Nutrients* 2018;**10**:1631. https://doi.org/10.3390/nu10111631
23. Mujica-Coopman MF, Farias DR, Franco-Sena AB. *et al.* Maternal plasma pyridoxal 5′-phosphate concentration is inversely associated with plasma cystathionine concentration across all trimesters in healthy pregnant women. *J Nutr* 2019;**149**:1354–62. https://doi.org/10.1093/jn/nxz082
24. Nobakht M, Gh BF. Application of metabolomics to preeclampsia diagnosis. *Syst Biol Reprod Med* 2018;**64**:324–39. https://doi.org/10.1080/19396368.2018.1482968
25. Bahado-Singh RO, Akolekar R, Mandal R. *et al.* Metabolomics and first-trimester prediction of early-onset preeclampsia. *J Matern Fetal Neonatal Med* 2012;**25**:1840–7.
26. Kyozuka H, Fukuda T, Murata T. *et al.* Comprehensive metabolomic analysis of first-trimester serum identifies biomarkers of early-onset hypertensive disorder of pregnancy. *Sci Rep* 2020;**10**:13857. https://doi.org/10.1038/s41598-020-70974-3
27. Carter RA, Pan K, Harville EW. *et al.* Metabolomics to reveal biomarkers and pathways of preterm birth: a systematic review and epidemiologic perspective. *Metabolomics* 2019;**15**:124. https://doi.org/10.1007/s11306-019-1587-1
28. Considine EC, Khashan AS, Kenny LC. Screening for preterm birth: potential for a metabolomics biomarker panel. *Metabolites* 2019;**9**:90. https://doi.org/10.3390/metabo9050090
29. Lee SM, Kang Y, Lee EM. *et al.* Metabolomic biomarkers in midtrimester maternal plasma can accurately predict the development of preeclampsia. *Sci Rep* 2020;**10**:16142. https://doi.org/10.1038/s41598-020-72852-4
30. Lowe WL, Karban J. Genetics, genomics and metabolomics: new insights into maternal metabolism during pregnancy. *Diabet Med* 2014;**31**:254–62. https://doi.org/10.1111/dme.12352

31. Petrick L, Edmands W, Schiffman C. *et al.* An untargeted metabolomics method for archived newborn dried blood spots in epidemiologic studies. *Metabolomics* 2017;**13**:27. https://doi.org/10.1007/s11306-016-1153-z
32. Handelman SK, Romero R, Tarca AL. *et al.* The plasma metabolome of women in early pregnancy differs from that of non-pregnant women. *PloS One* 2019;**14**:e0224682. https://doi.org/10.1371/journal.pone.0224682
33. Ghaemi MS, DiGiulio DB, Contrepois K. *et al.* Multiomics modeling of the immunome, transcriptome, microbiome, proteome and metabolome adaptations during human pregnancy. *Bioinformatics* 2018;**35**:95–103. https://doi.org/10.1093/bioinformatics/bty537
34. Pirhaji L, Milani P, Leidl M. *et al.* Revealing disease-associated pathways by network integration of untargeted metabolomics. *Nat Methods* 2016;**13**:770–6. https://doi.org/10.1038/nmeth.3940
35. Price ND, Magis AT, Earls JC. *et al.* A wellness study of 108 individuals using personal, dense, dynamic data clouds. *Nat Biotechnol* 2017;**35**:747–56. https://doi.org/10.1038/nbt.3870
36. Shen X, Kellogg R, Panyard DJ. *et al.* Multi-omics microsampling for the profiling of lifestyle-associated changes in health. *Nat Biomed Eng* 2024;**8**:12–29. https://doi.org/10.1038/s41551-022-00999-8.
37. Shen X, Yan H, Wang C. *et al.* TidyMass an object-oriented reproducible analysis framework for LC–MS data. *Nat Commun* 2022;**13**:4365. https://doi.org/10.1038/s41467-022-32155-w
38. Shen X, Wu S, Liang L. *et al.* metID: an R package for automatable compound annotation for LC–MS-based data. *Bioinformatics* 2022;**38**:568–9. https://doi.org/10.1093/bioinformatics/btab583
39. Shen X, Wang C, Snyder MP. massDatabase: utilities for the operation of the public compound and pathway database. *Bioinformatics* 2022;**38**:4650–1. https://doi.org/10.1093/bioinformatics/btac546
40. Djoumbou Feunang Y, Eisner R, Knox C. *et al.* ClassyFire: automated chemical classification with a comprehensive, computable taxonomy. *J Chem* 2016;**8**:61. https://doi.org/10.1186/s13321-016-0174-y
41. Edwards DP, O'Conner JL, Bransome ED. *et al.* Human placental 3beta-hydroxysteroid dehydrogenase: Delta5-isomerase. Demonstration of an intermediate in the conversion of 3beta-hydroxypregn-5-en-20-one to pregn-4-ene-3,20-dione. *J Biol Chem* 1976;**251**:1632–8. https://doi.org/10.1016/S0021-9258(17)33695-5
42. Solano ME, Arck PC. Steroids, pregnancy and fetal development. *Front Immunol* 2020;**10**:3017. https://doi.org/10.3389/fimmu.2019.03017
43. Czyzyk A, Podfigurna A, Genazzani AR. *et al.* The role of progesterone therapy in early pregnancy: from physiological role to therapeutic utility. *Gynecol Endocrinol* 2017;**33**:421–4. https://doi.org/10.1080/09513590.2017.1291615
44. Romero R, Conde-Agudelo A, da Fonseca E. *et al.* Vaginal progesterone for preventing preterm birth and adverse perinatal outcomes in singleton gestations with a short cervix: a meta-analysis of individual patient data. *Am J Obstet Gynecol* 2018;**218**:161–80. https://doi.org/10.1016/j.ajog.2017.11.576
45. Jarde A, Lutsiv O, Beyene J. *et al.* Vaginal progesterone, oral progesterone, 17-OHPC, cerclage, and pessary for preventing preterm birth in at-risk singleton pregnancies: an updated systematic review and network meta-analysis. *BJOG* 2019;**126**:556–67. https://doi.org/10.1111/1471-0528.15566
46. Conde-Agudelo A, Romero R, da Fonseca E. *et al.* Vaginal progesterone is as effective as cervical cerclage to prevent preterm birth in women with a singleton gestation, previous spontaneous preterm birth, and a short cervix: updated indirect comparison meta-analysis. *Am J Obstet Gynecol* 2018;**219**:10–25. https://doi.org/10.1016/j.ajog.2018.03.028
47. Norman JE. Progesterone and preterm birth. *Int J Gynaecol Obstet Off Organ Int Fed Gynaecol Obstet* 2020;**150**:24–30. https://doi.org/10.1002/ijgo.13187
48. Kim SS, Mendola P, Zhu Y. *et al.* Spontaneous and indicated preterm delivery risk is increased among overweight and obese women without prepregnancy chronic disease. *BJOG* 2017;**124**:1708–16. https://doi.org/10.1111/1471-0528.14613
49. Cnattingius S, Villamor E, Johansson S. *et al.* Maternal obesity and risk of preterm delivery. *JAMA* 2013;**309**:2362–70. https://doi.org/10.1001/jama.2013.6295
50. Howell KR, Powell TL. Effects of maternal obesity on placental function and fetal development. *Reprod Camb Engl* 2017;**153**:R97–108.
51. Jelliffe-Pawlowski LL, Norton ME, Baer RJ. *et al.* Gestational dating by metabolic profile at birth: a California cohort study. *Am J Obstet Gynecol* 2016;**214**:511.e1. https://doi.org/10.1016/j.ajog.2015.11.029
52. Aghaeepour N, Ganio EA, Mcilwain D. *et al.* An immune clock of human pregnancy. *Sci Immunol* 2017;**2**:eaan2946. https://doi.org/10.1126/sciimmunol.aan2946
53. Peterson LS, Stelzer IA, Tsai AS. *et al.* Multiomic immune clockworks of pregnancy. *Semin Immunopathol* 2020;**42**:397–412. https://doi.org/10.1007/s00281-019-00772-1
54. Matteson KA, Rahn DD, Wheeler TL 2nd. *et al.* Nonsurgical management of heavy menstrual bleeding: a systematic review. *Obstet Gynecol* 2013;**121**:632–43. https://doi.org/10.1097/AOG.0b013e3182839e0e
55. van der Linden M, Buckingham K, Farquhar C. *et al.* Luteal phase support for assisted reproduction cycles. *Cochrane Database Syst Rev* 2015;**2015**:CD009154. https://doi.org/10.1002/14651858.CD009154.pub3
56. Munro MG, Critchley HOD, Fraser IS. *et al.* The FIGO classification of causes of abnormal uterine bleeding in the reproductive years. *Fertil Steril* 2011;**95**:2208.e1–3. https://doi.org/10.1016/j.fertnstert.2011.03.079
57. Yamauchi T, Ochi D, Matsukawa N. *et al.* Machine learning approaches to predict gestational age in normal and complicated pregnancies via urinary metabolomics analysis. *Sci Rep* 2021;**11**:17777. https://doi.org/10.1038/s41598-021-97342-z
58. Contrepois K, Chen S, Ghaemi MS. *et al.* Prediction of gestational age using urinary metabolites in term and preterm pregnancies. *Sci Rep* 2022;**12**:8033. https://doi.org/10.1038/s41598-022-11866-6
59. Tarca AL, Pataki BÁ, Romero R. *et al.* Crowdsourcing assessment of maternal blood multi-omics for predicting gestational age and preterm birth. *Cell Rep Med* 2021;**2**:100323. https://doi.org/10.1016/j.xcrm.2021.100323
60. Hrydziuszko O, Viant MR. Missing values in mass spectrometry based metabolomics: An undervalued step in the data processing pipeline. *Metabolomics* 2012;**8**:161–74. https://doi.org/10.1007/s11306-011-0366-4
61. Tusher VG, Tibshirani R, Chu G. Significance analysis of microarrays applied to the ionizing radiation response. *Proc Natl Acad Sci* 2001;**98**:5116–21. https://doi.org/10.1073/pnas.091062498
62. Shen X, Yan H, Wang C. *et al.* TidyMass an object-oriented reproducible analysis framework for LC-MS data. *Nat Commun* 2022;**13**:4365. https://doi.org/10.1038/s41467-022-32155-w
63. Viant MR, Kurland IJ, Jones MR. *et al.* How close are we to complete annotation of metabolomes? *Curr Opin Chem Biol* 2017;**36**:64–9. https://doi.org/10.1016/j.cbpa.2017.01.001

Briefings in Bioinformatics, 2025, **26(1)**, bbaf059
https://doi.org/10.1093/bib/bbaf059
Case Study